

Quantum model for Impulsive Stimulated Raman Scattering

Filippo Glerean,¹ Stefano Marcantoni,^{1,2} Giorgia Sparapassi,¹ Andrea Blason,¹ Martina Esposito,³ Fabio Benatti,^{1,2,*} and Daniele Fausti^{1,4,†}

¹*Dipartimento di Fisica, Università degli studi di Trieste, Via Valerio 2 Trieste 34127, Italy*

²*Istituto Nazionale di Fisica Nucleare, Sezione di Trieste, Trieste 34014, Italy*

³*Clarendon Laboratory, Department of Physics, University of Oxford, Oxford OX1 3PU, United Kingdom*

⁴*Sincrotrone Trieste S.C.p.A., Basovizza 34127, Italy*

(Dated: July 19, 2022)

The interaction between ultrashort light pulses and non-absorbing materials is dominated by Impulsive Stimulated Raman Scattering (ISRS). The description of ISRS in the context of pump&probe experiments is based on effective classical models describing the interaction between the phonon and pulsed electromagnetic fields. Here we report a theoretical description of ISRS where we do not make any semi-classical approximation and we treat both photonic and phononic degrees of freedom at the quantum level. The results of the quantum model are compared with semiclassical results and validated by means of spectrally resolved pump&probe measurements on α -quartz.

I. INTRODUCTION

The excitation and measurements of coherent lattice (or molecular) vibrations in time domain experiments relies on the possibility of using ultrashort optical pulses in pairs, one as a pump and a second as a probe. The pump should be capable of injecting energy into the phonon modes on time scales shorter than the inverse of the phonon frequency, while the probe should be short enough to measure the time evolution of this state with time. In this limit, photoexcitation produces coherent vibrational states whose dissipative dynamics can be directly accessed by pump&probe experiments [1–8].

The processes for transferring energy from the optical pulse to the phonons depends strongly on the nature of the material. In absorbing systems, the whole light-matter interaction processes should be described taking into account that the dissipative dynamics affecting the photo-excited electrons, which mediate the energy transfer from the light pulse to lattice excitations, may play a crucial role [9–15]. The situation is simpler in “transparent materials”, i.e. in materials where there is no dipole allowed electronic transitions available in the frequency range of the ultrashort pulses. In this limit, the interaction between the latter and the vibrational modes is a coherent process, where dissipative electron dynamics can be neglected and the whole process can be described effectively as a direct coupling between the ultrashort pulses and the phonon modes.

In this limit the interaction is dominated by processes dubbed Impulsive Stimulated Raman Scattering (ISRS) [16, 17]. ISRS takes place whenever a sufficiently short laser pulse (i.e. characterized by a multimode frequency spectrum larger than the phonon frequency) propagates through a Raman-active medium. In this limit, components of the electric field at different frequency can inter-

act through ISRS if the difference between their photon energy matches the energy of a phonon mode. More formally, ISRS can be described as a coherent process mixing three frequencies¹ where the stimulated annihilation (creation) of a photon of frequency ω occurs simultaneously to the creation (annihilation) of one at frequency $\omega \pm \Omega$. The overall process can create (Stokes) or annihilate (anti-Stokes) an excitation in the system and thereby result in lattice excitations. Note that in literature the term ISRS is often used to describe the whole pump and probe measurement process, while here we use it solely to indicate the physical process describing photon-phonon interaction. We will apply ISRS separately to describe how coherent lattice vibrations can be produced (pump) and measured (probe) by ISRS.

In this paper we study the leading processes occurring in a pump&probe experiment in transparent materials. From the interaction energy, given as a scalar product of the electric and the polarization fields, we construct the quantum Raman Hamiltonian which rules the bulk dynamics. In addition to this, we consider a modulation of the refractive index of the material that we refer to as Linear Refractive Modulation (LRM). The acronym highlights the fact that LRM consists of a “Linear”² interaction of the probe with a material whose Refractive index is Modulated in time by the evolving atomic position. We stress that while ISRS is a non-linear process coupling different spectral components of the pulses, LRM does not mix different probe frequencies.

Our approach provides a formalism to describe the fundamental differences between the ISRS and the LRM. As sketched in Fig.1, LRM amounts to a modulation of the

¹ The process occurs simultaneously between all pairs of frequencies and therefore the resulting electric field at frequency ω is influenced by both the electric field components at $\omega \pm \Omega$.

² We note that the overall process is describing non-linear responses in the susceptibility, but the term “linear” is used to clarify that no frequency mixing of the probe spectral components occurs.

* benatti@ts.infn.it

† daniele.fausti@elettra.eu

refractive index induced by the instantaneous position of the atoms (phonon position operator, q) which does not couple different photonic mode operators (a_j), but induces a change in transmittivity which is uniform with respect to the spectral components. Conversely, ISRS is a nonlinear process that produces a shift of the spectral weights relative to different photonic modes in the probe pulses [18] and follows the phonon momentum operator, p . ISRS and LRM give rise to a time-oscillation of the response with the same frequency but shifted in phase and, more importantly, with different spectral content. The two processes are often observed simultaneously and can result in composite responses. We validate the proposed quantum model by comparing the results with those obtained by classical calculations [19, 20] and with the outcomes of pump&probe experiments in α -quartz providing time and spectral resolution of the probe pulses. Further, we show that it is possible to disentangle experimentally LRM and ISRS effects in pump&probe experiments by selecting a proper combination of polarizations exploiting the symmetry of the crystal [21].

The paper is structured as follows. In section II we describe the quantum model for light-matter interaction. In particular, we distinguish between the peculiar characteristics of LRM and ISRS not always recognized in the literature [20, 22]. In section III we apply the general model already discussed in the context of pump&probe experiments, highlighting similarities and differences between the pumping and the probing processes, mainly due to the different vibrational target states before the photon-phonon interaction. In section IV the results are validated by means of spectrally resolved pump&probe experiments on α -quartz, where combination between pump and probe polarizations allow for the experimentally accessible distinction of ISRS and LRM processes. Finally, we conclude with some remarks and new perspectives offered by the fully quantum treatment of time-domain experiments [6, 23–26].

II. LIGHT-PHONON INTERACTION

A dielectric medium is polarized by an electromagnetic wave propagating through it. The components of the polarization field \vec{P} are expressed in terms of the impinging electric field \vec{E} and the material susceptibility tensor χ :

$$P_\lambda = \epsilon_0 \sum_{\lambda'} \chi_{\lambda\lambda'} E_{\lambda'}, \quad (1)$$

where ϵ_0 is the electric permittivity of the vacuum. One of the fundamental ingredients of the whole discussion is the susceptibility tensor dependence on the lattice deformations, i.e. those caused by excited vibrational modes. Considering tiny displacements out of the equilibrium position, the susceptibility can be perturbatively expanded around its initial value $\chi^{(0)}$ as a function of the lattice normal modes coordinates q_n , also referred to as phonon

positions (n labels the mode) [27, 28]:

$$\chi_{\lambda\lambda}(q_1, \dots, q_N) = \chi_{\lambda\lambda}^{(0)} + \sum_n \chi_{\lambda\lambda}^{(1)}(n) q_n. \quad (2)$$

where we defined $\chi_{\lambda\lambda}^{(1)}(n) := \left(\delta\chi / \delta q_n \right)_{\chi_{\lambda\lambda}}|_{q_n=0}$ the components of the rank three non-linear susceptibility tensor $\chi^{(1)}$.

In order to simplify the notation, in the following we neglect the summation over n and discuss the interaction of a single phononic mode with light. The characteristic structure of different modes will be highlighted in the last part of the paper, where we consider the specific case of quartz and compare the experimental evidences with the model predictions.

As a consequence of the refractive index dependence on the susceptibility, $\mathbf{n} = \sqrt{1 + \chi}$, a first effect is the modulation of the refractive properties at the material surface as a function of the phonon position operator to be introduced below. It can modify both transmitted intensity and polarization, while it does not imply an exchange of energy between the light and the sample. In the following, we model this interaction, the LRM effect, with an appropriate beam-splitter Hamiltonian H_{Ref} .

Another effect, the ISRS effect, emerges considering the bulk energy exchange between the solid and the light. The energy density required to establish the polarization \vec{P} in a dielectric sample is given by [28]

$$\begin{aligned} U(\vec{x}, t) &= -\vec{P}(\vec{x}, t) \cdot \vec{E}(\vec{x}, t) \\ &= -\epsilon_0 \sum_{\lambda\lambda'} \chi_{\lambda\lambda'} E_{\lambda'}(\vec{x}, t) E_\lambda(\vec{x}, t). \end{aligned} \quad (3)$$

From this expression, substituting the susceptibility as in (2) and quantizing the electric field, we derive (see Supplementary Material) the quantum Raman interaction Hamiltonian H_{Ram} that will be used in the following, together with a phonon independent equilibrium term, which we do not consider in our approach [29].

The system dynamics is obtained acting impulsively with the refractive Hamiltonian H_{Ref} and, subsequently, with the Raman Hamiltonian H_{Ram} for times short with respect to the scale determined by the Raman coefficients, such that a perturbative treatment is justified.

Concerning the initial states, we describe the impinging light pulse as a multimode coherent state $|\alpha\rangle$, where α stands for the vector with components $\alpha_{\lambda j}$, given by

$$|\alpha\rangle = \exp\left(\sum_{\lambda,j} \alpha_{\lambda j} a_{\lambda j}^\dagger - \alpha_{\lambda j}^* a_{\lambda j}\right) |0\rangle, \quad a_{\lambda j} |\alpha\rangle = \alpha_{\lambda j} |\alpha\rangle, \quad (4)$$

with annihilation and creation operators of photonic modes $a_{\lambda j}$ and $a_{\lambda j}^\dagger$ such that $[a_{\lambda j}, a_{\lambda' k}^\dagger] = \delta_{jk} \delta_{\lambda\lambda'}$, where $|0\rangle$ is the vacuum state and λ, j are the polarization and frequency indices, respectively. In particular, we consider a set of modes centered around the frequency ω_0 and spaced by δ : $\omega_j = j\delta + \omega_0$.

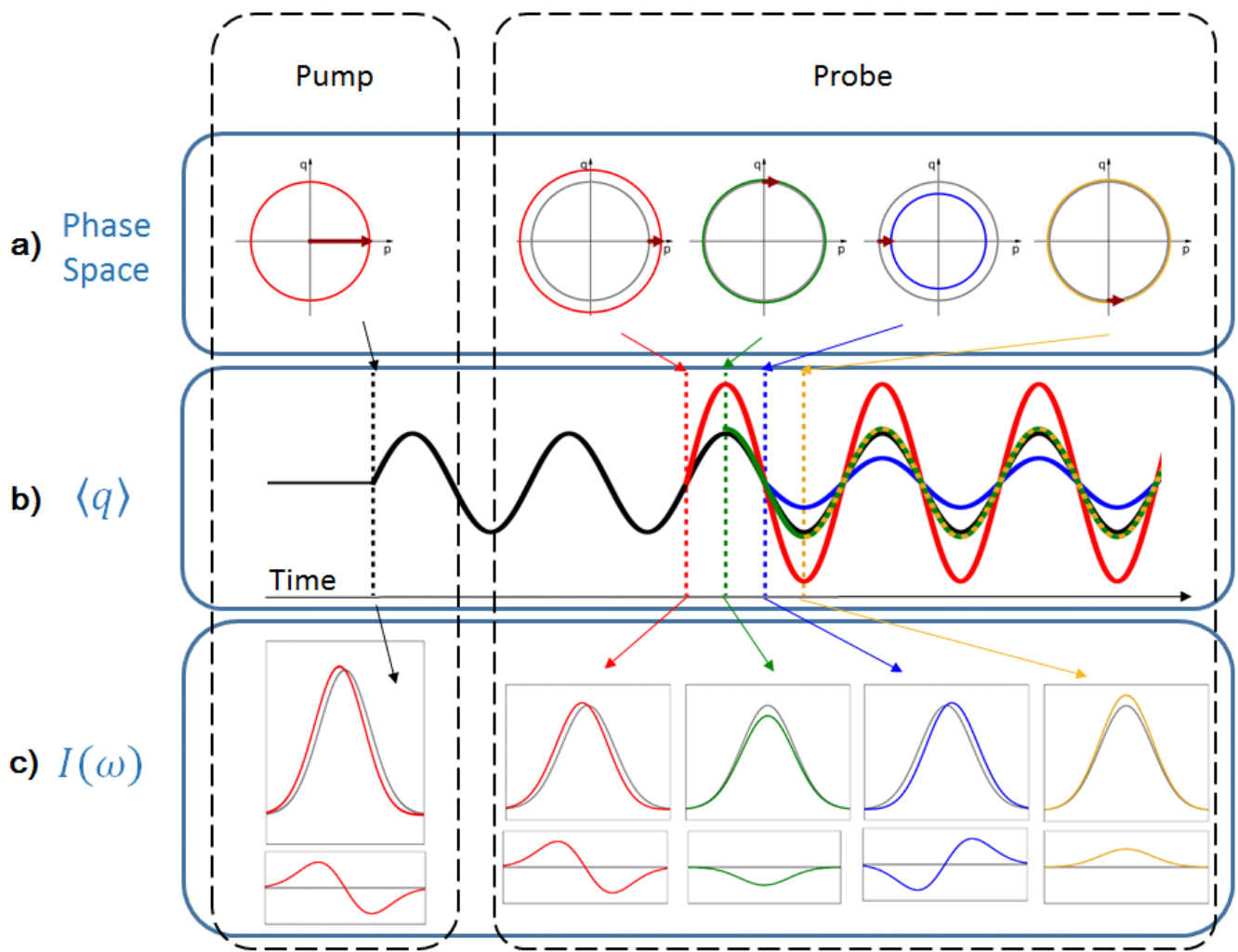


FIG. 1. Summary of the predicted effects. a) Pump and probe induced displacements (arrow) describe the effect on the vibrational energy ($\frac{\langle p^2 \rangle}{2m} + \frac{1}{2}m\Omega^2 \langle q^2 \rangle$). Depending on the phase space coordinates at the interaction time the phonon oscillation (b) can be amplified (red) or damped (blue). The corresponding effect on the transmitted pulse spectra (c) is a *red-shift* or *blue-shift*, respectively. The energy exchange is most important at the momentum extremes. At the extremal positions the oscillation is negligibly amplified and the relevant effect is a modulation of the transmittivity which does not change the spectral content (green and gold).

The phononic degree of freedom, (we provide the general model considering only one vibrational mode), is instead described through the operators b and b^\dagger , satisfying the commutation relation $[b, b^\dagger] = 1$. Accordingly, the position and momentum phonon operators mentioned above are defined as linear combinations of b and b^\dagger :

$$q = \frac{1}{\sqrt{2m\Omega V_S}}(b + b^\dagger), \quad p = \sqrt{\frac{m\Omega}{2V_S}}i(b^\dagger - b), \quad (5)$$

where Ω is the frequency of the mode, m is the effective mass and V_S is the volume of the sample. Using this notation, in the following we discuss separately the two different effects, LRM and ISRS, commenting on how they modify the transmitted light and the phononic phase-space.

A. Refractive modulation

In the quantum scheme that we are going to present, the redistribution of photons between reflected and transmitted beams at the sample surface is described through the following beam-splitter Hamiltonian H_{Ref} :

$$H_{Ref} = \sum_{\lambda\lambda',j} T_{\lambda\lambda'} \left(a_{\lambda j}^\dagger r_{\lambda'j} + a_{\lambda j} r_{\lambda'j}^\dagger \right), \quad (6)$$

where the annihilation operators $a_{\lambda j}$ refer to the transmitted light, while $r_{\lambda j}$ to the reflected radiation. The refractive properties are specified by the tensor \mathbf{T} , which depends on the phonon position through the refractive index and susceptibility. In particular, we consider a first order expansion of the matrix \mathbf{T} , in analogy with (2),

and assume that the correction to the transmission matrix, say $\mathbf{T}^{(1)}$, is proportional to $\chi^{(1)}$ through a constant k_T ,

$$T_{\lambda\lambda'} = T_{\lambda\lambda'}^{(0)} + k_T \chi_{\lambda\lambda'}^{(1)} \langle q \rangle, \quad (7)$$

where $\mathbf{T}^{(0)}$ is the transmission matrix at equilibrium, that is without phonon excitation, and we highlight the linear dependence on the mean value of the normal mode phonon position operator q (5). The average $\langle q \rangle$ is computed with respect to the initial state of the phonons, corresponding to the instant of time at which the light beam impinges the sample. Assuming both matrices $\mathbf{T}^{(0)}$ and $\chi^{(1)}$ to be real symmetric, the occupation numbers (i.e. the intensity $I_{\lambda j} = a_{\lambda j}^\dagger a_{\lambda j}$) of the transmitted light after refraction at the sample surface read

$$\langle I_{\lambda j} \rangle = \sum_{\lambda'\lambda''} C_{\lambda\lambda'} C_{\lambda\lambda''} |\alpha_{\lambda'j}| |\alpha_{\lambda''j}|, \quad (8)$$

where $C_{\lambda\lambda'}$ are the matrix elements of $\mathbf{C} = \cos(\mathbf{T})$, defined through the cosine power series. In the supplementary material, more details about the derivation of (8) are given, where we also compute explicitly the coefficients $C_{\lambda\lambda'}$ by assuming a particular form for the matrix \mathbf{T} . In the rest of the paper, we will then use approximated expressions up to first order in $\langle q \rangle$, namely

$$C_{\lambda\lambda'} = C_{\lambda\lambda'}^{(0)} + C_{\lambda\lambda'}^{(1)} \langle q \rangle. \quad (9)$$

B. Impulsive Stimulated Raman Scattering

The interaction in the bulk of the sample is modelled by the Raman Hamiltonian that is derived from the quantization of the dipole energy (3):

$$H_{Ram} = -\frac{\sqrt{V_S}}{2V\sqrt{2m\Omega}} \sum_{\lambda\lambda',j} \omega_j \chi_{\lambda\lambda'}^{(1)} \left[\left(a_{\lambda j}^\dagger a_{\lambda'j+\frac{\Omega}{8}} \right) b^\dagger + \left(a_{\lambda j} a_{\lambda'j+\frac{\Omega}{8}}^\dagger \right) b \right], \quad (10)$$

where V_S and V are the sample and quantization volumes, respectively, Ω the phonon frequency, m its effective mass and ω_j the photon frequencies. The non-linear susceptibility coefficients $\chi_{\lambda\lambda'}^{(1)}$ are assumed real, such that $\chi_{\lambda\lambda'}^{(1)} = \chi_{\lambda'\lambda}^{(1)}$, and small in absolute value. Considering the photonic (a) and phononic (b) ladder operators, in the two terms of H_{Ram} we clearly observe the Stokes and Anti-Stokes nature. Photons with energy ω_j and polarization λ are destroyed by $a_{\lambda j}$ and photons of energy $\omega_j \pm \Omega$ and polarization λ' are created by $a_{\lambda'j\pm\frac{\Omega}{8}}^\dagger$, together with the emission (b^\dagger) and annihilation (b) of a phonon, respectively.

The expressions presented in the following for the mean values of some relevant observables are obtained considering a phase matching condition between the photonic modes of the laser beam. This assumption corresponds to the maximal efficiency of the Raman process and gives a straightforward physical representation in the phononic phase-space. More details regarding the phase dependence are given in the Supplementary Material.

We consider the pulse propagation inside the sample starting at time 0 up to time τ , shorter than the phonon oscillation period. As explicitly shown in the Supplementary Material, the evolution of the phononic operator b in this time-interval, and up to first order in the small parameters of the processes involved, reads as follows

$$b(\tau) = b(0) + i \frac{\tau \sqrt{V_S}}{2V\sqrt{2m\Omega}} g, \quad (11)$$

$$\text{where } g = \sum_{\lambda\lambda',j} \chi_{\lambda\lambda'}^{(1)} \omega_j a_{\lambda j}^\dagger a_{\lambda'j+\frac{\Omega}{8}}.$$

With this expression for $b(\tau)$ we can calculate the resulting mean values of the phonon phase-space variables position q and momentum p , with respect to a generic initial state:

$$\begin{cases} \langle q(\tau) \rangle = \langle q(0) \rangle, \\ \langle p(\tau) \rangle = \langle p(0) \rangle + \frac{\tau}{2V} \gamma, \end{cases} \quad (12)$$

$$\text{with } \gamma = \langle g \rangle = \sum_{\lambda\lambda',j} \chi_{\lambda\lambda'}^{(1)} \omega_j |\alpha_{\lambda j}| |\alpha_{\lambda'j+\frac{\Omega}{8}}|.$$

We observe that the effect of the Raman interaction is a displacement along the momentum axis, as depicted in Fig. 2, where the squared radius R^2 gives the mean value of the phonon number $N = b^\dagger b$, which to second order in the $\tau \chi^{(1)}$ coupling parameter results

$$\langle N(\tau) \rangle = \langle N(0) \rangle + \frac{\tau V_S}{2V m \Omega} \gamma \langle p(0) \rangle + \frac{\tau^2 V_S}{8V^2 m \Omega} \langle g^\dagger g \rangle. \quad (13)$$

We notice that the first order contribution depends on the value of the momentum p before the interaction, while the second order term is proportional to the mean value of the operator $g^\dagger g$, which equals γ^2 if light states are classical (coherent states such that $|\alpha|^2 \gg 1$). The second order term is usually negligible with respect to the first one unless $\langle p(0) \rangle = 0$.

The effects on the phononic degrees of freedom have their counterparts on the photonic ones. The intensity of the transmitted light at a certain frequency ω_j and polarization λ , computed as $\langle I_{\lambda j}(\tau) \rangle := \langle a_{\lambda j}^\dagger(\tau) a_{\lambda j}(\tau) \rangle$ reads

$$\begin{aligned} \langle I_{\lambda j}(\tau) \rangle &= \langle I_{\lambda j}(0) \rangle \\ &+ \frac{\tau V_S}{2V m \Omega} \sum_{\lambda} \chi_{\lambda\lambda}^{(1)} \omega_j |\alpha_{\lambda j}| \\ &\times \left(|\alpha_{\lambda j+\frac{\Omega}{8}}| - |\alpha_{\lambda j-\frac{\Omega}{8}}| \right) \left(\langle p(0) \rangle + \frac{\tau}{4V} \gamma \right) \\ &+ \tau^2 \gamma'_j \end{aligned} \quad (14)$$

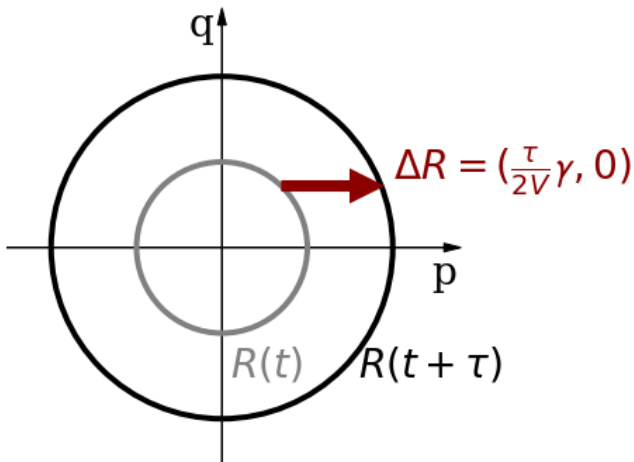


FIG. 2. Phase space representation of the Raman interaction between light and phonon. The circular trajectory is the one followed by the free evolution of the coherent phonon, modelled as an harmonic oscillator. Light-phonon imparts a positive momentum displacement (arrow) modifying the radius of the phonon trajectory.

where the first order contribution again depends on $\langle p(0) \rangle$ and is related to the difference in amplitude between the modes corresponding to the frequencies $\omega_j + \Omega$ and $\omega_j - \Omega$. Among the second order terms, one can recognize a term with a similar structure, where the dependence on $\langle p(0) \rangle$ is substituted by γ , and a further contribution γ'_j which depends on the mean-values of squared phonon operators. All the details can be found in the Supplementary Material.

Equipped with this general machinery, we now proceed to study in detail the quantum signatures in pump&probe experiments.

III. PUMP AND PROBE APPROACH

Pump&probe experiments provide standard techniques in time-resolved spectroscopy, whereby a first intense laser pulse (the pump) excites the vibrational degrees of freedom of a sample and a second pulse, less intense, is used to probe non-equilibrium features. By repeating the experiment at different time-delays between pump and probe, one can retrieve information about the phonon dynamics in the sample.

In the following, we describe how the theoretical model presented in the previous section applies in this framework, highlighting the different effects due to the pump and the probe pulses. We will consider the pump acting on the phononic equilibrium state at a reference time $t = 0$, and study the probe response as a function of the delay time t . In particular, we focus on frequency and polarization resolved intensity measurements, that we can describe through the equations ruling the LRM (8) and

ISRS (14) effects.

A. Pump-target interaction

We assume the pump impinging on the sample at equilibrium, where the phononic position and momentum have zero average $\langle q(0) \rangle = \langle p(0) \rangle = 0$. This is the case for instance if the initial state of the vibrational degrees of freedom has a thermal distribution. According to equation (42), without any modulation of the refractive index ($\langle q(0) \rangle = 0$), the transmitted intensity just before the bulk interaction starts, namely right after the refraction at the boundary, reads

$$\langle I_{\lambda j}^{pump}(0) \rangle_0 = |\tilde{\alpha}_{\lambda j}^{pump}|^2, \quad \tilde{\alpha}_{\lambda j}^{pump} = \sum_{\lambda'} C_{\lambda \lambda'}^{(0)} \alpha_{\lambda' j}^{pump}, \quad (15)$$

where the zero subscript denotes the pump impinging time, the one in the brackets the time at which the bulk propagation starts, and $\tilde{\alpha}_{\lambda j}^{pump}$ are the amplitudes of the coherent state produced by the refraction acting on the initial photon coherent state with amplitudes $\alpha_{\lambda j}^{pump}$. The ISRS effect on the intensity is then evaluated considering $\tilde{\alpha}_{\lambda j}^{pump}$ as input in (14). The first order term is null because of $\langle p(0) \rangle = 0$ and we also neglect the term γ_j^{pump} because the phonon population is negligible with respect to the photon number. The result is

$$\langle I_{\lambda j}^{pump}(\tau) \rangle_0 = |\tilde{\alpha}_{\lambda j}^{pump}|^2 + \frac{\tau^2 v_s^2}{8v^2 m \Omega} \tilde{\gamma}^{pump} \sum_{\lambda} \chi_{\lambda \lambda}^{(1)} \omega_j |\tilde{\alpha}_{\lambda j}^{pump}| \left(|\tilde{\alpha}_{\lambda j + \frac{\Omega}{8}}^{pump}| - |\tilde{\alpha}_{\lambda j - \frac{\Omega}{8}}^{pump}| \right), \quad (16)$$

which can be interpreted as an effective red-shift of the pulse spectrum. Indeed, assuming the incoming pulse to have a Gaussian spectrum centered in ω_0 , equation (16) implies that modes with frequency smaller than that ω_0 are amplified (because the difference $|\tilde{\alpha}_{\lambda j + \frac{\Omega}{8}}^{pump}| - |\tilde{\alpha}_{\lambda j - \frac{\Omega}{8}}^{pump}|$ is positive), while modes with frequency higher than ω_0 are suppressed.

Correspondingly, according to (12), the phonon system is shifted from the origin of the phase space ($\langle q(0) \rangle_0 = 0, \langle p(0) \rangle_0 = 0$) along the momentum axis to a trajectory of radius

$$R \equiv \langle p(\tau) \rangle_0 = \frac{\tau}{2V} \tilde{\gamma}^{pump}. \quad (17)$$

B. Probe-target interaction

We consider the probe interacting at an arbitrary delay-time t . Considering that the excitation starts when the pump interacts ($t = 0$), at negative times the probe still sees the system in equilibrium. Afterwards, the considered phonon mode is excited and the sample starts oscillating at the corresponding phonon frequency Ω . In

the following, we neglect dissipative effects occurring in the time-interval between the action of the two pulses, the evolution being described by the Hamiltonian of a free quantum harmonic oscillator. As a consequence, the initial conditions for the probe interaction are:

$$\begin{cases} t < 0, & \langle q(0) \rangle_t = \langle p(0) \rangle_t = 0 \\ t > 0, & \langle q(0) \rangle_t = \frac{R}{m\Omega} \sin(\Omega t), \quad \langle p(0) \rangle_t = R \cos(\Omega t). \end{cases} \quad (18)$$

In the following we consider only positive delay-times $t > 0$.

Combining the refractive (8) and Raman (14) contributions, we obtain an explicit expression for the resulting intensity as a function of phonon position and momentum,

$$\begin{aligned} \langle I_{\lambda j}^{probe}(\tau) \rangle_t &= |\tilde{\alpha}_{\lambda j}^{probe}|^2 \\ &+ 2 \sum_{\lambda' \lambda''} |\alpha_{\lambda' j}^{probe}| |\alpha_{\lambda'' j}^{probe}| C_{\lambda \lambda'}^{(0)} C_{\lambda \lambda''}^{(1)} \langle q(0) \rangle_t \\ &+ \frac{\tau V_S}{2V m \Omega} \sum_{\lambda} \chi_{\lambda \lambda}^{(1)} \omega_j |\tilde{\alpha}_{\lambda j}^{probe}| \left(|\tilde{\alpha}_{\lambda j + \frac{\Omega}{\delta}}^{probe}| - |\tilde{\alpha}_{\lambda j - \frac{\Omega}{\delta}}^{probe}| \right) \langle p(0) \rangle_t, \end{aligned} \quad (19)$$

where we have safely neglected the second order ISRS terms considering that $\gamma^{probe} \ll \langle p(0) \rangle_t$ due to $|\alpha^{pump}| \gg |\alpha^{probe}|$.

We will use this expression as a benchmark for the model, comparing the predicted results with experimental data for the probe transmitted intensity.

IV. CASE STUDY: QUARTZ

In the model developed so far, we considered only one phononic mode of frequency Ω . Actually the generalization to many phononic modes is straightforward, the calculations being more involved though. However, since we are interested only in the first order corrections to the transmittivity of the probe pulse, we can safely add the contribution of different phononic modes independently. In other words, coupling between different phononic modes would be a higher order effect. The case study we are going to discuss is that of α -quartz excited along its c -axis [30, 31]. In this setting, three different symmetry classes come into play for the phononic modes depending on the geometry of the pump-probe polarization [21]. These three classes correspond to specific properties of the susceptibility tensor. In particular, for the classes called A (totally symmetric), and the two degenerate E_L (longitudinal) and E_T (transverse), $(\chi_n^{(1)})_{\lambda \lambda}$ has the form

$$A = \begin{pmatrix} a & 0 \\ 0 & a \end{pmatrix}, \quad E^L = \begin{pmatrix} c_L & 0 \\ 0 & -c_L \end{pmatrix}, \quad E^T = \begin{pmatrix} 0 & -c_T \\ -c_T & 0 \end{pmatrix}. \quad (20)$$

In the following, by varying the angle between the pump and the probe polarization, we discuss the transmittivity dependence on the symmetry classes.

A. Model prediction

In order to make quantitative predictions, we fix specific features of the pulses. Both pump and probe are chosen to be linearly polarized laser beams with a Gaussian spectrum of height $\alpha_0 > 0$

$$\alpha_j = \alpha_0 e^{-(j\delta)^2/(2\sigma^2)}, \quad (21)$$

where σ is the width of the pulse frequency distribution. The difference in intensity between pump and probe is accounted for by setting $|\alpha_0^{pump}| \gg |\alpha_0^{probe}|$. We consider a reference frame such that the probe is initially polarized along the x axis while the pump is oriented at an angle θ with respect to it. In order to make the dependence on θ explicit, we choose the initial state of the pump such that $a_{\lambda j} |\alpha^{pump}\rangle = \alpha_{\lambda j}^{pump} |\alpha^{pump}\rangle$ where

$$\alpha_{xj}^{pump} = \alpha_j^{pump} \cos(\theta), \quad \alpha_{yj}^{pump} = \alpha_j^{pump} \sin(\theta). \quad (22)$$

The transmittivity of the probe after the action of the pump depends on the radial parameter R introduced in (68), which, according to our model, contains all the information about the phonon dynamics. In particular, it turns out that

$$\begin{aligned} R_A &= a \tilde{\eta}_{\Omega_A}^{pump}, \\ R_{E^L} &= c_L \cos(2\theta) \tilde{\eta}_{\Omega_E}^{pump}, \\ R_{E^T} &= -c_T \sin(2\theta) \tilde{\eta}_{\Omega_E}^{pump}, \end{aligned} \quad (23)$$

where the parameter $\tilde{\eta}_{\Omega}^{pump}$ has been defined as follows

$$\tilde{\eta}_{\Omega}^{pump} = \frac{\tau}{2V} \sum_j \omega_j |\tilde{\alpha}_j^{pump}| |\tilde{\alpha}_{j+\frac{\Omega}{\delta}}^{pump}|. \quad (24)$$

When the analyzer selects the polarization along the x axis, the transmitted intensity reads

$$\begin{aligned} \langle I_{xj}^{probe}(\tau) \rangle_t &= \langle I_{xj}^{probe}(0) \rangle_0 \\ &- 2k_T |\tilde{\alpha}_j^{probe}|^2 \left[a^2 \frac{\tilde{\eta}_{\Omega_A}^{pump}}{m_A \Omega_A} \sin(\Omega_A t) \right. \\ &+ c_L^2 \cos(2\theta) \frac{\tilde{\eta}_{\Omega_E}^{pump}}{m_E \Omega_E} \sin(\Omega_E t) \\ &+ c_T^2 \sin(2\theta) \frac{\tilde{\eta}_{\Omega_E}^{pump}}{m_E \Omega_E} T_{xy}^{(0)} \sin(\Omega_E t) \left. \right] \\ &+ \frac{\tau V_S}{2V} \omega_j |\tilde{\alpha}_j^{probe}| \left[a^2 \left(|\tilde{\alpha}_{j+\frac{\Omega_A}{\delta}}^{probe}| - |\tilde{\alpha}_{j-\frac{\Omega_A}{\delta}}^{probe}| \right) \frac{\tilde{\eta}_{\Omega_A}^{pump}}{m_A \Omega_A} \cos(\Omega_A t) \right. \\ &+ c_L^2 \cos(2\theta) \left(|\tilde{\alpha}_{j+\frac{\Omega_E}{\delta}}^{probe}| - |\tilde{\alpha}_{j-\frac{\Omega_E}{\delta}}^{probe}| \right) \frac{\tilde{\eta}_{\Omega_E}^{pump}}{m_E \Omega_E} \cos(\Omega_E t) \left. \right], \end{aligned} \quad (25)$$

while, choosing the polarization along the y axis yields

$$\begin{aligned} \langle I_{yj}^{probe}(\tau) \rangle_t &= \\ &+ \frac{2k_T}{m_E \Omega_E} |\tilde{\alpha}_j^{probe}|^2 T_{xy}^{(0)} c_T^2 \sin(2\theta) \tilde{\eta}_{\Omega_E}^{pump} \sin(\Omega_E t). \end{aligned} \quad (26)$$

We summarize here some basic conclusions that can be drawn from the previous equations and which are compatible with the existing classical descriptions present in the literature [19, 20]:

- Different modes of vibration in the crystal are excited depending on the polarization angle of the pump pulse. This fact is described by the presence of the parameter θ in the model.
- The LRM effect does not couple different modes of light and produces a global amplitude modulation (8), whereas the Raman process gives a shift in the spectral weight, preserving the total intensity (14).
- For a given phononic mode, the modification of the transmittivity produced by the displacement dependent LRM effect oscillates in time with a different phase with respect to the momentum dependent ISRS effect. In particular, when the Raman effect is maximum the refractive modulation is zero and viceversa, so that it is possible to distinguish the two processes looking at specific time-delays between pump and probe.

B. Experiment

What is measured in pump&probe experiments is the modulation of the probe transmitted intensity $\langle \Delta I_{\lambda_j}^{probe} \rangle_t = \langle I^{probe}(\tau)_{\lambda_j} \rangle_t - \langle I^{probe}(\tau)_{\lambda_j} \rangle_{<0}$, as a function of the pump&probe delay and frequency-resolved over the pulse spectrum; the experimental outcome can thus be compared with the theoretical prediction obtained by means of the expression (19). Furthermore, by adjusting the experimental parameters, one can select the pump orientation θ and the analyzed polarization λ . The experimental setup details are given in the supplementary material [32]. The employed pulse fluences are 0.8 mJ/cm^2 for the pump and $0.7 \mu\text{J/cm}^2$ for the probe.

In this section we present two peculiar configurations, the particular geometry of which is useful to discuss and verify the main predicted features and distinguish LRM and ISRS effects. We consider the reference frame in IV A and present the data normalized by the unperturbed (negative times) peak intensity $\langle I^{probe}(\tau)_{x0} \rangle_{<0}$. We obtain the phonon frequencies performing the Fourier Transform (FT) of the positive delays and we focus on the spectral shape of the modulation at relevant times. We set the zero delay at the centre of the overlap between pump and probe pulses (which last about 40 fs)³.

Firstly, the pump is polarized along the x axis too, $\theta = 0^\circ$, and the transmitted light is measured in the parallel polarization. According to the theoretical model,

both the A mode and the E_L mode contribute to the dynamics and the ISRS as well as the LRM effects are visible. This is consistent with the experimental evidence as shown in Fig.9. We notice in the phonon spectrum the presence of both A and E symmetry peaks and we highlight the ISRS red/blue-shift modulations. In the second

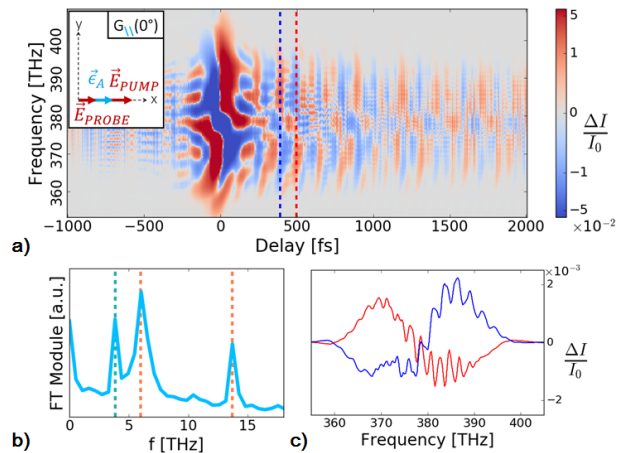


FIG. 3. Results depending on the relative orientation between pump and probe polarizations and analyzer direction. a) Spectral modulation vs delay in the ($\lambda = x, \theta = 0^\circ$) configuration (insert) is presented. b) FT: 4 THz E_L phonon is detected, together with 6 THz and 14 THz A symmetry modes. c) The transmittivity modulation is selected at $t = 391$ fs (blue) and $t = 498$ fs (red). Spectral shifts resulting from ISRS are observed.

case (Fig.7), maintaining the probe oriented along x , the pump is rotated $\theta = 45^\circ$ and the analyzer is setted cross (y axis). The model correctly predicts that only the oscillation produced by the transverse mode is visible in the FT. In particular, as we observe modulations of the same sign along the full spectrum, we may conclude that this oscillation is produced by the LRM. Moreover, comparing figure 9 and 7 also the phase shift between ISRS and refractive effects is confirmed. The theoretical transmittivity, as predicted by (25)(26), is plotted in the two mentioned configurations in the supplementary material.

In addition to these configurations, we fully verify the symmetry properties by means of measurements for other values of θ . In figure 5 we show summary polar plots where we represent the peak intensity of the FT for a selected phonon as a function of the pump orientation and the selected polarization.

V. CONCLUSIONS

In conclusion, we presented a theoretical quantum model that describes the interactions between the vibrational degrees of freedom of a crystal (phonons) and a multimode light beam. Two different effects, not clearly distinguished in the literature, have been considered, namely the Impulsive Stimulated Raman Scattering and

³ Notice that around this region the interpretation is complicated by interference and other effects related to the pulse duration.

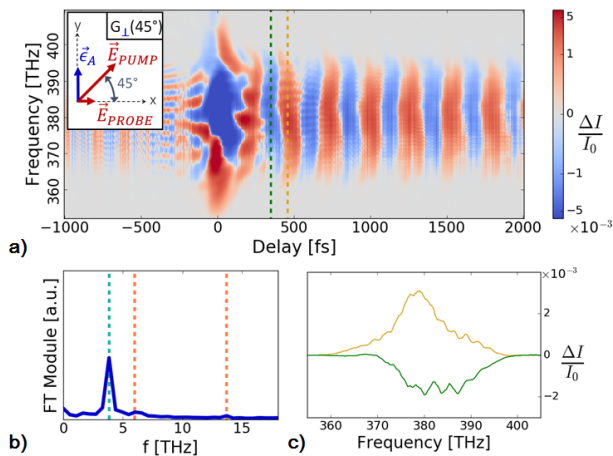


FIG. 4. a) Spectral modulation vs delay in the ($\lambda = y$, $\theta = 45^\circ$) configuration (insert) is presented. b) FT: only the 4 THz E_T phonon is detected. c) The transmittivity modulation is selected at $t = 351$ fs (green) and $t = 458$ fs (gold). As expected for the refractive modulation the transmittivity change has the same sign for the whole spectrum.

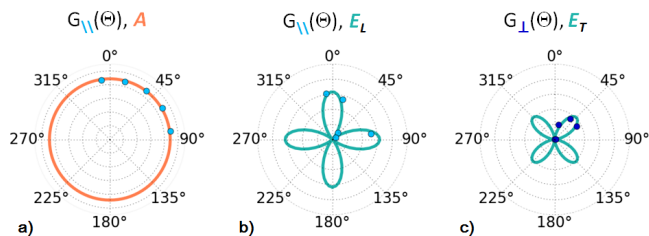


FIG. 5. Polar plots representative of the different phonon symmetries are presented for an analyzer setted parallel (a,b) or orthogonal (cross) (c) to the probe polarization. Measured signal intensity (dots) for each considered mode is fitted (line) with the proper dependence on relative orientation between pump&probe, suggested by (23). a) A -mode 6 THz, b) E^L -mode 4 THz phonon, parallel polarization. c) E^T -mode 4 THz phonon, cross polarization.

the Linear Refractive Modulation. The model is applied to the description of pump&probe experiments, where a first intense laser pulse is used to excite the vibrations in a sample and then a second light beam is used to probe the dynamics of these vibrations, highlighting the different features in the two situations. In particular, for experiments based on α -quartz, in different geometrical settings the theoretical predictions agree with the experimental findings. Though the results are compatible with classical descriptions of light-matter interaction, the quantum model can be applied to more general situations, where one is interested in ISRS-induced multi-mode correlations and classical models can fail. In this respect, this paper should be seen as a first benchmark on the quality of our model which can be further exploited in the context of different measurements unveiling purely quantum effects. Moreover, it can be used as a tool to

infer the non-equilibrium properties of complex materials via spectroscopic measurement.

ACKNOWLEDGMENTS

This work was partially supported by the European Research Council through the Grant Agreement No. 677488. F.G., G.S., M.E. and D.F. worked on the pump-probe experiment with quartz, while F.G., S.M., A.B. and F.B. developed the theoretical model.

F.G. and S.M. contributed equally to this work.

-
- [1] M. Hase, K. Mizoguchi, H. Harima, S. Nakashima, M. Tani, K. Sakai, M. Hangyo, *Optical control of coherent optical phonons in Bismuth films*, Appl. Phys. Lett., 69(17), 24742476 (1996).
- [2] M. Hase, M. Kitajima, S. Nakashima, K. Mizoguchi, *Dynamics of coherent phonons in Bismuth generated by ultrashort laser pulses*, Phys. Rev. B, 58(9), 54485452 (1998).
- [3] M. Hase, M. Kitajima, S. Nakashima, K. Mizoguchi, *Dynamics of Coherent Anharmonic Phonons in Bismuth Using High Density Photoexcitation*, Phys. Rev. Lett., 88, 067401 (2002).
- [4] M. F. DeCamp, D. A. Reis, P.H. Bucksbaum, R. Merlin, *Dynamics and coherent control of high-amplitude optical phonons in Bismuth*, Phys. Rev. B, 64, 092301 (2001).
- [5] S. Fahy, D. A. Reis, *Coherent Phonons: Electronic Softening or Anharmonicity?*, Phys. Rev. Lett., 93, 109701 (2004).
- [6] O.V. Misochko, *Coherent Phonons and Their Properties*, Journal of Experimental and Theoretical Physics, 92(2), 246-259 (2001).
- [7] K. Ishioka, M. Kitajima, O.V. Misochko, *Temperature dependence of coherent A_{1g} and E_g phonons in Bismuth*, J. Appl. Phys., 100, 093501 (2006).
- [8] O.V. Misochko, K. Ishioka, M. Hase, M. Kitajima, *Fano interference for large amplitude coherent phonons in Bismuth*, J. Phys. Condensed Matter, 19(15), 156227 (2007).
- [9] H. J. Zeiger, J. Vidal, T. K. Cheng, E. P. Ippen, G. Dresselhaus, M. S. Dresselhaus, *Theory for dispersive excitation of coherent phonons*, Phys. Rev. B, 45(2), 768778 (1992).
- [10] G. A. Garrett, T. F. Albrecht, J. F. Whitaker, R. Merlin, *Coherent THz Phonons Driven by Light Pulses and the Sb Problem: What is the Mechanism?*, Phys. Rev. Lett., 77(17), 3661 (1996).
- [11] T. E. Stevens, J. Kuhl, R. Merlin, *Coherent phonon generation and the two stimulated Raman tensors*, Phys. Rev. B, 65, 144304 (2002).
- [12] D. Fausti, O. Misochko, P. Van Loosdrecht, *Ultrafast photoinduced structure phase transition in antimony single crystals*, Phys. Rev. B, 80, 161207 (2009).
- [13] E. Papalazarou, J. Faure, J. Mauchain, M. Marsi, A. Taleb-Ibrahimi, I. Reshetnyak, A. van Roekeghem, I. Timrov, N. Vast, B. Arnaud, L. Perfetti, *Coherent Phonon Coupling to Individual Bloch States in Photoexcited Bismuth*, Phys. Rev. Lett., 108, 256808 (2012).
- [14] F. Randi, M. Esposito, F. Giusti, O. Misochko, F. Parmigiani, D. Fausti, and M. Eckstein, *Probing the Fluctuations of Optical Properties in Time-Resolved Spectroscopy*, Phys. Rev. Lett. 119, 187403 (2017).
- [15] M. Ruggenthaler, N. Tancogne-Dejean, J. Flick, H. Appel, A. Rubio, *From a quantum-electrodynamical light-matter description to novel spectroscopies*, Nature Reviews Chemistry 2, 0118 (2018).
- [16] Y.X. Yan, E.B. Gamble, K.A. Nelson, *Impulsive stimulated scattering: General importance in femtosecond laser pulse interactions with matter, and spectroscopic applications*, J. Chem. Phys. 83, 5391 (1985).
- [17] Y.X. Yan, K.A. Nelson, *Impulsive stimulated light scattering. I. General theory*, J. Chem. Phys. 87, 6240 (1987).
- [18] K.G. Nakamura et al., *Spectrally resolved detection in transient-reflectivity measurements of coherent optical phonons in diamond*, Phys. Rev. B 94, 024303 (2016).
- [19] R. Merlin, *Generating coherent THz phonons with light pulses*, Solid State Commun. 102(2-3), 207-220 (1997).
- [20] L. Dhar, J.A. Rogers, K.A. Nelson, *Time-Resolved Vibrational Spectroscopy in the Impulsive Limit*, Chem. Rev. 94, 157-193 (1994).
- [21] A. Rundquist, J. Broman, D. Underwood, D. Blank, *Polarization-dependent detection of impulsive stimulated Raman scattering in α -quartz*, Journal of Modern Optics 52 (17), 25012510 (2005).
- [22] R. Righini, *Ultrafast Optical Kerr Effect in Liquids and Solids*, Science 262 (5138), 1386-1390 (1993).
- [23] H. Xu, F. Nori, *Phonon Squeezed States Generated by Second-Order Raman Scattering*, Phys. Rev. Lett. 79(23), 4605 (1997).
- [24] H. Xu, F. Nori, *Phonon squeezed states: quantum noise reduction in solids*, Physica B, 263-264, 16-29 (1999).
- [25] M. Esposito, K. Titimbo, K. Zimmermann, F. Giusti, F. Randi, D. Boschetto, F. Parmigiani, R. Floreanini, F. Benatti, D. Fausti, *Phonon number statistics uncover the fluctuations in non-equilibrium lattice dynamics*, Nature Communication 6, 10249 (2015).
- [26] A. Hussain, S. R. Andrews, *Absence of phase-dependent noise in time-domain reflectivity studies of impulsively excited phonons*, Phys. Rev. B 81, 224304 (2010).
- [27] E.O. Potma, S. Mukamel, *Theory of Coherent Raman Scattering*, Coherent Raman Scattering Microscopy, edited by J.X. Cheng and X.S. Xie (CRC Press, Boca Raton, 2013), Chap. 1.
- [28] R. Boyd, *Nonlinear Optics* (Academic Press, 2007), Third Edition.
- [29] A. Blason, *Teoria Quantistica dello Scattering Raman Impulsato e Stimolato*, Bachelor thesis, Universit degli Studi di Trieste (2017).
- [30] J. F. Scott and S. P. S. Porto, *Longitudinal and transverse optical lattice vibrations in quartz.*, Phys. Rev. 161, 903 (1967).
- [31] M.M. Wefers, H. Kawashima, K.A. Nelson, *Optical control over two-dimensional lattice vibrational trajectories in crystalline quartz*, J. Chem. Phys. 108, 10248 (1998).
- [32] F. Glerean, *Noise Correlation Spectroscopy for Impulsive Stimulated Raman Scattering*, Master thesis, Universit degli Studi di Trieste (2017).

Supplementary material

QUANTUM MODEL

A full quantum description of the pulse-target photon-phonon interaction can be provided by assuming the process to consist of two independent, that is dynamically decoupled contributions:

1. an instantaneous refraction process at the interface between target and the incoming laser pulse that rotates the polarization of the latter (we called this process Linear Refractive Modulation, LRM, in the main text);
2. Raman Stokes and anti-Stokes processes affecting the transmitted photons while they cross the target and interact with its vibrational degrees of freedom (Impulsive Stimulated Raman Scattering, ISRS, in the main text).

These processes act in succession on an incoming mode-locked laser pulse consisting of linearly polarized photons with frequencies $\omega_j = \omega_0 + j\delta$, $-J \leq j \leq J$, described by a coherent state

$$|\alpha\rangle = \exp\left(\sum_{j,\lambda} \alpha_{\lambda j} a_{\lambda j}^\dagger - \alpha_{\lambda j}^* a_{\lambda j}\right)|0\rangle, \quad a_{\lambda j}|\alpha\rangle = \alpha_{\lambda j}|\alpha\rangle, \quad (27)$$

with annihilation and creation operators $a_{\lambda j}$ and $a_{\lambda j}^\dagger$ such that $[a_{\lambda j}, a_{\lambda' k}^\dagger] = \delta_{jk}\delta_{\lambda\lambda'}$, where $|0\rangle$ is the vacuum state, $\lambda = x, y$ are polarization indices and j a frequency index. The $N = 2J + 1$ frequencies $\omega_j = \omega_0 + j\delta$ are distributed around a central frequency ω_0 with δ a constant depending on the laser repetition rate. Furthermore, we will consider an ω_0 centered, Gaussian shaped pulse so that, together with the mode-locking condition on the phases of the contributing amplitudes ($\varphi_j = j\varphi' + \varphi_0$),

$$\alpha_{\lambda j} = \alpha_\lambda e^{-(j\delta)^2/(2\sigma^2)} e^{i(j\varphi' + \varphi_0)}, \quad (28)$$

where $\alpha_\lambda > 0$ and φ' is the mode-locking reference phase and σ is the width of the frequency distribution in the pulse.

For sake of simplicity, the vibrational properties of the target will be described by a single phonon mode of energy Ω associated with bosonic annihilation and creation operators b and b^\dagger such that $[b, b^\dagger] = 1$.

Physical justification of the model

In the following we present some considerations in order to physically justify the model we are considering. First, we discuss the refractive contribution and explain why we can relate this phenomenon to a beam splitter Hamiltonian. Then, we derive the Raman Hamiltonian from the dipole energy density.

Refraction

When a light beam impinges an interface between two different materials, part of the light is reflected and part is transmitted and, in general, the polarization of both the transmitted and reflected beams can change with respect to the one of the incident light. The equations describing the amplitude and polarization of the light beams are the Fresnel equations, which in turn can be derived from the Maxwell equations in matter. For anisotropic materials the transmission and reflection coefficients are somehow involved expressions containing the refraction index tensor \mathbf{n} , that is related to the susceptibility χ as follows

$$\mathbf{n}^2 = 1 + \chi. \quad (29)$$

Moreover, the susceptibility χ varies in time due to the phonons excited in the material, so that one can think to expand the susceptibility in power series with respect to the phonon coordinate $q_n(\vec{x})$ (n labels the different modes). Up to first order one has

$$\chi = \chi^{(0)} + \sum_n \chi_n^{(1)} q_n(\vec{x}), \quad (30)$$

so that the Fresnel coefficients will also depend on the phonon position. In order to effectively describe the refraction process we use a beam splitter hamiltonian where the matrix of coefficients can be expanded up to first order in the phonon-position mean-values $\langle q \rangle$.

Raman

The Raman interaction Hamiltonian can be derived from the dipole energy density that reads

$$U^{\text{int}}(\vec{x}) = -\epsilon_0 \sum_{\lambda\lambda'} \chi_{\lambda\lambda'} E_\lambda(\vec{x}) E_{\lambda'}(\vec{x}) = -\epsilon_0 \sum_{\lambda\lambda'} \left(\chi_{\lambda\lambda'}^{(0)} + \sum_n \chi_{n;\lambda\lambda'}^{(1)} q_n(\vec{x}) \right) E_\lambda(\vec{x}) E_{\lambda'}(\vec{x}), \quad (31)$$

where the elastic field $q_n(\vec{x})$ describing the vibration in the crystal, together with its momentum $p_n(\vec{x})$, and the electric field $E_\lambda(\vec{x})$ polarized along λ can be quantized as follows

$$E_\lambda(\vec{x}) = i \sum_j \sqrt{\frac{\omega_j}{2V\epsilon_0}} \left(a_{\lambda j} e^{-i(\omega_j t - \vec{k}_j \cdot \vec{x})} - a_{\lambda j}^\dagger e^{i(\omega_j t - \vec{k}_j \cdot \vec{x})} \right), \quad (32)$$

$$q_n(\vec{x}) = \frac{1}{\sqrt{2m_n\Omega_n V_S}} \left(b_n^\dagger e^{i(\Omega_n t - \vec{u}_n \cdot \vec{x})} + b_n e^{-i(\Omega_n t - \vec{u}_n \cdot \vec{x})} \right), \quad (33)$$

$$p_n(\vec{x}) = i \sqrt{\frac{m_n\Omega_n}{2V_S}} \left(b_n^\dagger e^{i(\Omega_n t - \vec{u}_n \cdot \vec{x})} - b_n e^{-i(\Omega_n t - \vec{u}_n \cdot \vec{x})} \right). \quad (34)$$

In writing the previous expressions we used \vec{u}_n, \vec{k}_j for the vibration and electric field wave vectors, respectively, Ω_n, ω_j are the frequencies of the lattice vibration and electric field, m_n is the effective mass of the n th normal mode, V is the quantization volume of the electric field and V_S is the volume of the sample. The interaction Hamiltonian without any approximation is therefore obtained integrating $U^{\text{int}}(\vec{x})$ over the volume of the sample and reads

$$\mathcal{H}_{\text{int}} = \int_{V_S} d\vec{x} \epsilon_0 \sum_{\lambda\lambda'} \left[\chi_{\lambda\lambda'}^{(0)} + \sum_n \chi_{n;\lambda\lambda'}^{(1)} \frac{1}{\sqrt{2m_n\Omega_n V_S}} \left(b_n^\dagger e^{i(\Omega_n t - \vec{u}_n \cdot \vec{x})} + b_n e^{-i(\Omega_n t - \vec{u}_n \cdot \vec{x})} \right) \right] \times \quad (35)$$

$$\times \sum_{j\ell} \frac{\sqrt{\omega_j\omega_\ell}}{2V\epsilon_0} \left(a_{\lambda j} e^{-i(\omega_j t - \vec{k}_j \cdot \vec{x})} - a_{\lambda j}^\dagger e^{i(\omega_j t - \vec{k}_j \cdot \vec{x})} \right) \left(a_{\lambda'\ell} e^{-i(\omega_\ell t - \vec{k}_\ell \cdot \vec{x})} - a_{\lambda'\ell}^\dagger e^{i(\omega_\ell t - \vec{k}_\ell \cdot \vec{x})} \right). \quad (36)$$

Assuming periodic boundary conditions, the integration of the \vec{x} -dependent terms, gives Kronecker deltas describing conservation of momentum

$$\int_{V_S} d\vec{x} e^{i(\vec{k}_j - \vec{k}_\ell - \vec{u}_n) \cdot \vec{x}} = V_S \delta_{\vec{k}_j, \vec{k}_\ell + \vec{u}_n}. \quad (37)$$

By concentrating on long wavelength phonons (with respect to the photon one), such that $u_n \simeq 0$, the problem becomes unidimensional because the wave-vector of the incident photon coincides with the wave-vector of the emitted photon. We can label the axis containing all the wave-vectors as z . Finally, by means of the rotating wave approximation we get rid of the terms like aa or $a^\dagger a^\dagger$ and all the terms $a_{\lambda j}^\dagger a_{\lambda'\ell}$ where $\omega_j - \omega_\ell \neq \Omega$. In the end, we get the Raman Hamiltonian

$$H_{\text{Ram}} = \sum_{\lambda\lambda',j} \omega_j \tilde{\chi}_{\lambda\lambda'}^{(1)} \left[\left(a_{\lambda j}^\dagger a_{\lambda'j+\frac{\Omega}{\omega_j}} \right) b^\dagger + \left(a_{\lambda j} a_{\lambda'j+\frac{\Omega}{\omega_j}} \right) b \right], \quad \tilde{\chi}_{\lambda\lambda'}^{(1)} = -\frac{\sqrt{V_S}}{2V\sqrt{2m\Omega}} \chi_{\lambda\lambda'}^{(1)}, \quad (38)$$

plus an equilibrium term that we do not consider in the rest of the paper,

$$H^0 = -\frac{V_S}{2V} \sum_{\lambda,\lambda';j} \chi_{\lambda\lambda'}^{(0)} a_{\lambda j}^\dagger a_{\lambda'j} + h.c. \quad (39)$$

In writing (44) we used the approximation $\sqrt{\omega_j(\omega_j \pm \Omega)} \sim \omega_j$, which is justified because in the following we are considering phononic frequencies in the range $350 \text{ THz} < \omega_j < 410 \text{ THz}$ while $\Omega < 10 \text{ THz}$.

Dynamics

The photon-phonon interactions at the boundary and in the bulk change the initial state $|\alpha\rangle\langle\alpha| \otimes \varrho$ according to

$$|\alpha\rangle\langle\alpha| \otimes \varrho \mapsto \Gamma_\tau \left[|\alpha\rangle\langle\alpha| \otimes \varrho \right] = U_{Ram}(\tau) \left(U_{Ref} |\alpha\rangle\langle\alpha| U_{Ref}^\dagger \otimes \varrho \right) U_{Ram}^\dagger(\tau), \quad (40)$$

where τ is the photon travel time in the bulk, ϱ is a quantum state for the vibrational degrees of freedom and U_{Ref} and U_{Ram} are the evolution operators describing the refractive and Raman modulation respectively, that we present in the following.

Refraction (LRM)

The unitary operator U_{Ref} affects only the photon degrees of freedom and describes an instantaneous refraction process at the boundary generating transmitted and reflected photons. The former are described by annihilation and creation operators $r_{\lambda j}$ and $r_{\lambda j}^\dagger$, $[r_{\lambda j}, r_{\lambda' k}^\dagger] = \delta_{jk} \delta_{\lambda\lambda'}$, while the latter by the incoming operators $a_{\lambda j}$, $a_{\lambda j}^\dagger$:

$$U_{Ref} = \exp(-i H_{Ref}), \quad H_{Ref} = \sum_{\lambda\lambda', j} T_{\lambda\lambda'} \left(a_{\lambda j}^\dagger r_{\lambda' j} + a_{\lambda j} r_{\lambda' j}^\dagger \right). \quad (41)$$

In the Hamiltonian H_{Ref} , the refraction index, which rules the splitting matrix \mathbf{T} , is assumed to be weakly modulated by the vibrational state of the target so that the refraction coefficients can be grouped into a matrix

$$\mathbf{T} = \mathbf{T}^{(0)} + \mathbf{T}^{(1)} \langle q \rangle, \quad \langle q \rangle = \frac{1}{\sqrt{2m\Omega V_S}} \langle b + b^\dagger \rangle = \frac{1}{\sqrt{2m\Omega V_S}} \text{Tr}(\varrho(b + b^\dagger)), \quad (42)$$

where $\mathbf{T}^{(1)}$ provides a perturbative term proportional to the mean value of the normal mode phonon position operator q with respect to the initial state ϱ . Both matrices $\mathbf{T}^{(0)}$ and $\mathbf{T}^{(1)}$ are assumed to be real symmetric. From (30), the position dependent modification is linearly coupled to $\chi^{(1)}$ and we consider in the following $\mathbf{T}^{(1)} = k_T \chi^{(1)}$, where k_T is a suitable proportionality factor.

The refraction process at the boundary acts only on the coherent photon part $|\alpha\rangle\langle\alpha|$ of the initial state: with respect to the whole set of photon operators a_{xj} , a_{yj} , r_{xj} and r_{yj} the coherent state $|\alpha\rangle$ can be expressed in terms of an amplitude vector α with $N = 2J + 1$ four-dimensional components $\alpha_j = (\alpha_{xj}, \alpha_{yj}, 0, 0)$. The refractive process transforms the coherent state $|\alpha\rangle$ into a new coherent state with non zero transmitted and reflected amplitudes for both polarizations:

$$U_{ref} |\alpha\rangle = |\tilde{\alpha}\rangle, \quad \tilde{\alpha}_j = (\alpha_{xj}^{tr}, \alpha_{yj}^{tr}, \alpha_{xj}^{ref}, \alpha_{yj}^{ref}), \quad \alpha_{\lambda j}^{ref} = -i \sum_{\lambda'} S_{\lambda\lambda'} \alpha_{\lambda' j}, \quad \alpha_{\lambda j}^{tr} = \sum_{\lambda'} C_{\lambda\lambda'} \alpha_{\lambda' j}, \quad \lambda, \lambda' = x, y, \quad (43)$$

with proportionality coefficients $C_{\lambda\lambda'}$ and $S_{\lambda\lambda'}$, that are the matrix elements of $\mathbf{C} = \cos(\mathbf{T})$ and $\mathbf{S} = \sin(\mathbf{T})$.

Raman

The Raman Hamiltonian can be written as

$$H_{Ram} = \sum_{\lambda\lambda', j} \omega_j \tilde{\chi}_{\lambda\lambda'}^{(1)} \left[\left(a_{\lambda j}^\dagger a_{\lambda' j + \frac{\Omega}{8}} \right) b^\dagger + \left(a_{\lambda j} a_{\lambda' j + \frac{\Omega}{8}} \right) b \right], \quad \tilde{\chi}_{\lambda\lambda'}^{(1)} = -\frac{\sqrt{V_S}}{2V\sqrt{2m\Omega}} \chi_{\lambda\lambda'}^{(1)} \quad (44)$$

where the matrix $\tilde{\chi}^{(1)}$ is proportional to the susceptibility $\chi^{(1)}$. The first term describes a Stokes process, where one photon loses energy into a phonon, and its hermitian conjugate an anti-Stokes one. The coupling coefficients $\tilde{\chi}_{\mu\mu'}^{(1)}$ are assumed real, such that $\tilde{\chi}_{\mu\mu'}^{(1)} = \tilde{\chi}_{\mu'\mu}^{(1)}$, and small in absolute value, such that a perturbative treatment of the dynamics is justified. The time-evolution of an operator O under the action of the unitary propagator $U_{Ram}(\tau) = e^{-i\tau H_{Ram}}$ is given by

$$O(\tau) = U_{Ram}^\dagger(\tau) O U_{Ram}(\tau), \quad (45)$$

and up to second order in the Raman coupling one can write

$$O(\tau) \simeq O + i\tau [H_{Ram}, O] - \frac{\tau^2}{2} [H_{Ram}, [H_{Ram}, O]]. \quad (46)$$

The parameter τ indicates the time duration of the bulk process which depends on the width of the target.

In the following, we study the time-evolution of specific observables induced by the Raman Hamiltonian. The first example is the phononic operator b . For this operator the second order term, *i.e.* the double commutator in (46), turns out to be zero and the time-evolution reads

$$b(\tau) \simeq b + i\tau \frac{\sqrt{V_S}}{2V\sqrt{2m\Omega}} g, \quad g = \sum_{\lambda\lambda',j} \chi_{\lambda\lambda'}^{(1)} \omega_j a_{\lambda j}^\dagger a_{\lambda'j+\frac{\Omega}{\delta}}, \quad (47)$$

where the operator g has been introduced for future convenience. By taking the average with respect to a factorized state $|\alpha\rangle\langle\alpha| \otimes \varrho$, where ϱ is a generic density matrix for the phononic degrees of freedom and $|\alpha\rangle$ is a coherent state as described in (27) and (28), one obtains

$$\langle b(\tau) \rangle := \text{Tr} [(|\alpha\rangle\langle\alpha| \otimes \varrho) b(\tau)] = \langle b \rangle + i\tau \frac{\sqrt{V_S}}{2V\sqrt{2m\Omega}} \gamma, \quad \gamma = \langle g \rangle = \sum_{\lambda\lambda',j} \chi_{\lambda\lambda'}^{(1)} \omega_j |\alpha_{\lambda j}| |\alpha_{\lambda'j+\frac{\Omega}{\delta}}| e^{i\varphi'\frac{\Omega}{\delta}}. \quad (48)$$

In the main paper, the corresponding expression is evaluated considering the phase matching condition, namely $\varphi' = 0$, such that the phase is the same for all modes j and γ is a real number.

Using the previous result one can compute the mean phonon position which is proportional to $b + b^\dagger$ and discover that up to second order in the Raman coupling this is modified by a term dependent on the mode-locking phase

$$\langle q(\tau) \rangle = \frac{1}{\sqrt{2m\Omega V_S}} \left(\langle b(\tau) \rangle + \langle b^\dagger(\tau) \rangle \right) = \langle q(0) \rangle - \frac{\tau}{2V m \Omega} |\gamma| \sin \left(\varphi' \frac{\Omega}{\delta} \right), \quad (49)$$

that vanishes in the phase-matching condition as discussed in the main paper. The mean phonon momentum is instead shifted by an amount proportional to the interaction time τ that survives also under phase-matching conditions

$$\langle p(\tau) \rangle = i\sqrt{\frac{m\Omega}{2V_S}} \left(\langle b^\dagger(\tau) \rangle - \langle b(\tau) \rangle \right) = \langle p(0) \rangle + \frac{\tau}{2V} |\gamma| \cos \left(\varphi' \frac{\Omega}{\delta} \right). \quad (50)$$

Analogously, for the phonon number operator one can explicitly compute

$$N(\tau) = (b^\dagger b)(\tau) \simeq b^\dagger b + i\tau \sum_{\lambda\lambda',j} \tilde{\chi}_{\lambda\lambda'}^{(1)} \omega_j \left(a_{\lambda'j+\frac{\Omega}{\delta}}^\dagger a_{\lambda j} b - a_{\lambda j}^\dagger a_{\lambda'j+\frac{\Omega}{\delta}} b^\dagger \right) + \tau^2 \frac{V_S}{8V^2 m \Omega} g^\dagger g, \quad (51)$$

and the mean number of phonons after the Raman interaction is

$$\langle N(\tau) \rangle = \langle N(0) \rangle - i\tau \frac{\sqrt{V_S}}{2V\sqrt{2m\Omega}} |\gamma| \left(e^{-i\varphi'\frac{\Omega}{\delta}} \langle b \rangle - e^{i\varphi'\frac{\Omega}{\delta}} \langle b^\dagger \rangle \right) + \tau^2 \frac{V_S}{8V^2 m \Omega} \langle g^\dagger g \rangle. \quad (52)$$

Under pahse-matching conditions, the expression becomes

$$\langle N(\tau) \rangle = \langle N(0) \rangle + \frac{\tau V_S |\gamma|}{2V m \Omega} \langle p(0) \rangle + \tau^2 \frac{V_S}{8V^2 m \Omega} \langle g^\dagger g \rangle. \quad (53)$$

Concerning the photonic operators $a_{\mu j}$ the Raman evolution yields

$$a_{\mu j}(\tau) \simeq a_{\mu j} + i\tau [H_{Ram}, a_{\mu j}] - \frac{\tau^2}{2} [H_{Ram}, [H_{Ram}, a_{\mu j}]] + \dots$$

where the first order contribution reads

$$[H_{Ram}, a_{\mu j}] = - \sum_{\lambda} \tilde{\chi}_{\mu\lambda}^{(1)} \left((\omega_j) a_{\lambda j+\frac{\Omega}{\delta}} b^\dagger + (\omega_j - \Omega) a_{\lambda j-\frac{\Omega}{\delta}} b \right)$$

while the second order one has the form:

$$\begin{aligned} \left[H_{Ram}, \left[H_{Ram}, a_{\mu j} \right] \right] &= \sum_{\lambda \eta} \tilde{\chi}_{\mu \lambda}^{(1)} \tilde{\chi}_{\lambda \eta}^{(1)} \left((\omega_j + \Omega) \omega_j a_{\eta j + \frac{2\Omega}{8}} (b^\dagger)^2 + (\omega_j - \Omega)^2 a_{\eta j} b b^\dagger + \right. \\ &\quad \left. + (\omega_j)^2 a_{\eta j} b^\dagger b + (\omega_j - 2\Omega)(\omega_j - \Omega) a_{\eta j - \frac{2\Omega}{8}} b^2 \right) + \\ &\quad \left. + \sum_{\lambda \eta \eta' k} \tilde{\chi}_{\mu \lambda}^{(1)} \tilde{\chi}_{\eta \eta'}^{(1)}(\omega_k) \left((\omega_j - \Omega) a_{\eta k}^\dagger a_{\eta' k + \frac{\Omega}{8}} a_{\lambda j - \frac{\Omega}{8}} - (\omega_j) a_{\eta' k + \frac{\Omega}{8}} a_{\eta k} a_{\lambda j + \frac{\Omega}{8}} \right). \end{aligned}$$

By taking the average with respect to the state $|\alpha\rangle\langle\alpha| \otimes \varrho$, since the main contributions come from the terms with frequencies in the range $350 \text{ THz} < \omega_j < 410 \text{ THz}$ while $\Omega < 10 \text{ THz}$, one can safely assume $\omega_j + \Omega \sim \omega_j$ and simplify the previous expressions. This is also consistent with the approximation used in obtaining the Raman Hamiltonian. The average transmitted intensity $I_{\lambda j} = a_{\lambda j}^\dagger a_{\lambda j}$ therefore reads

$$\langle I_{\lambda j}(\tau) \rangle = \langle I_{\lambda j}(0) \rangle - \tau \sum_{\lambda} \tilde{\chi}_{\lambda \lambda}^{(1)} \omega_j |\alpha_{\lambda j}| \left(|\alpha_{\lambda j + \frac{\Omega}{8}}| - |\alpha_{\lambda j - \frac{\Omega}{8}}| \right) \left(i \left(e^{i\varphi' \frac{\Omega}{8}} \langle b^\dagger \rangle - e^{-i\varphi' \frac{\Omega}{8}} \langle b \rangle \right) + \tau \frac{\sqrt{V_S}}{2V\sqrt{2m\Omega}} |\gamma| \right) + \tau^2 \gamma'_j, \quad (54)$$

while, under phase-matching conditions,

$$\langle I_{\lambda j}(\tau) \rangle = \langle I_{\lambda j}(0) \rangle + \tau \frac{V_S}{2V m \Omega} \sum_{\lambda} \chi_{\lambda \lambda}^{(1)} \omega_j |\alpha_{\lambda j}| \left(|\alpha_{\lambda j + \frac{\Omega}{8}}| - |\alpha_{\lambda j - \frac{\Omega}{8}}| \right) \left(\langle p(0) \rangle + \frac{\tau \gamma}{4V} \right) + \tau^2 \gamma'_j, \quad (55)$$

where the momentum dependence of the first order term has been highlighted, as well as a second order term with a similar structure apart from a parameter γ replacing p and a further second order term, indicated by γ'_j , containing contributions of second order in the phononic operators. Explicitly,

$$\begin{aligned} \gamma'_j &= \sum_{\lambda \eta} \tilde{\chi}_{\mu \lambda}^{(1)} \tilde{\chi}_{\mu \eta}^{(1)} \omega_j^2 \left(|\alpha_{\lambda j + \frac{\Omega}{8}}| |\alpha_{\eta j + \frac{\Omega}{8}}| \langle b b^\dagger \rangle + |\alpha_{\lambda j - \frac{\Omega}{8}}| |\alpha_{\eta j - \frac{\Omega}{8}}| \langle b^\dagger b \rangle + |\alpha_{\lambda j - \frac{\Omega}{8}}| |\alpha_{\eta j + \frac{\Omega}{8}}| \left(e^{2i\varphi' \frac{\Omega}{8}} \langle (b^\dagger)^2 \rangle + e^{-2i\varphi' \frac{\Omega}{8}} \langle b^2 \rangle \right) \right) \\ &\quad - \frac{1}{2} \sum_{\lambda \eta} \tilde{\chi}_{\mu \lambda}^{(1)} \tilde{\chi}_{\lambda \eta}^{(1)} \omega_j^2 |\alpha_{\mu j}| \left(\left(|\alpha_{\eta j + \frac{2\Omega}{8}}| + |\alpha_{\eta j - \frac{2\Omega}{8}}| \right) \left(e^{2i\varphi' \frac{\Omega}{8}} \langle (b^\dagger)^2 \rangle + e^{-2i\varphi' \frac{\Omega}{8}} \langle b^2 \rangle \right) + 2 |\alpha_{\eta j}| \langle b b^\dagger + b^\dagger b \rangle \right). \quad (56) \end{aligned}$$

Pump and Probe

The previous model applies to both pump and probe pulses but different assumptions and approximations can be used in the two cases. Indeed, when the pump pulse impinges the sample the vibrations are not yet excited and there is no refractive modulation at the boundary.

Pump

Concerning the pump pulse, in order to make explicit the dependence of its action on the pump polarization angle with respect to the x axis, we choose the coherent initial state of the pump $|\alpha^{pump}\rangle$ such that $a_{xj} |\alpha^{pump}\rangle = \alpha_{xj}^{pump} |\alpha^{pump}\rangle$ and $a_{yj} |\alpha^{pump}\rangle = \alpha_{yj}^{pump} |\alpha^{pump}\rangle$ where

$$\alpha_{xj}^{pump} = \alpha_j^{pump} \cos(\theta), \quad \alpha_{yj}^{pump} = \alpha_j^{pump} \sin(\theta). \quad (57)$$

Moreover, we assume the state of the vibrational degree of freedom before the action of the pump to be a thermal state $\varrho_\beta = \frac{e^{-\beta \Omega b^\dagger b}}{\text{Tr}[e^{-\beta \Omega b^\dagger b}]}$ such that in the refraction matrix \mathbf{T} one has $\langle b + b^\dagger \rangle = 0$. Therefore, in this case there is no modulation of the refraction index, which is settled at the equilibrium value as described by $\mathbf{T}^{(0)}$.

The refraction process modifies the coherent state $|\alpha^{pump}\rangle$ into $|\tilde{\alpha}^{pump}\rangle$ according to (43). Then, the Raman interaction occurs as explained in the previous section, on an initial state of the form $|\tilde{\alpha}^{pump}\rangle \langle \tilde{\alpha}^{pump}| \otimes \varrho_\beta$. The first order Raman contribution to the transmitted intensity is vanishing because $\langle p(0) \rangle = 0$. As a result, the mean atomic displacement and its derivative have the form specified in the main text

$$\langle q(\tau) \rangle = 0, \quad \langle p(\tau) \rangle = \frac{\tau}{4V} \gamma^{pump}. \quad (58)$$

The mean number of phonons is modified by a second order contribution related to $(\gamma^{pump})^2$

$$\langle N(\tau) \rangle = \langle N(0) \rangle + \tau^2 \frac{V_S}{8V^2 m \Omega} \langle g^\dagger g \rangle, \quad (59)$$

while the light intensity reads

$$\langle I_{\lambda j}(\tau) \rangle = |\tilde{\alpha}_{\lambda j}^{pump}|^2 + \frac{\tau^2 V_S}{8V^2 m \Omega} \gamma^{pump} \sum_{\lambda} \chi_{\lambda\lambda}^{(1)} \omega_j |\tilde{\alpha}_{\lambda j}^{pump}| \left(|\tilde{\alpha}_{\lambda j + \frac{\Omega}{8}}^{pump}| - |\tilde{\alpha}_{\lambda j - \frac{\Omega}{8}}^{pump}| \right) + \tau^2 (\gamma_j^{pump})'. \quad (60)$$

Probe

We assume the probe pulse, impinging the target at delay-time t , to be polarized along the x axis so that the photon state is the coherent state $|\alpha^{probe}\rangle$ such that

$$a_{xj} |\alpha^{probe}\rangle = \alpha_j^{probe} |\alpha^{probe}\rangle, \quad a_{yj} |\alpha^{probe}\rangle = 0. \quad (61)$$

After the refraction process the coherent state $|\alpha^{probe}\rangle$ is modified into $|\tilde{\alpha}^{probe}\rangle$ and, as a consequence of (43) the following holds

$$a_{xj} |\tilde{\alpha}^{probe}\rangle = C_{xx} \alpha_j^{probe} |\tilde{\alpha}^{probe}\rangle, \quad a_{yj} |\tilde{\alpha}^{probe}\rangle = C_{xy} \alpha_j^{probe} |\tilde{\alpha}^{probe}\rangle. \quad (62)$$

On the other hand, the phonon state $\varrho(t)$ at delay-time t is the result of the pump action at $t = 0$ on the initial phonon thermal state ϱ_β and of its subsequent time-evolution up to time t which we assume to be free and thus described by the unitary operator

$$U_{free}(t) = e^{-i\Omega b^\dagger b t}. \quad (63)$$

Therefore

$$\varrho(t) = U_{free}(t) U_{Ram}(\tau) \varrho_\beta U_{Ram}^\dagger(\tau) U_{free}^\dagger(t),$$

whence the average $\langle b + b^\dagger \rangle_t$ reads

$$\langle b + b^\dagger \rangle_t = \text{Tr} \left[\varrho_\beta \left(e^{-i\Omega t} \left(b + i\tau \frac{\sqrt{V_S}}{2V \sqrt{2m\Omega}} \gamma^{pump} \right) + e^{i\Omega t} \left(b^\dagger - i\tau \frac{\sqrt{V_S}}{2V \sqrt{2m\Omega}} \gamma^{pump} \right) \right) \right] = \tau \frac{\sqrt{V_S}}{V \sqrt{2m\Omega}} \gamma^{pump} \sin(\Omega t), \quad (64)$$

inducing a modulation of the refractive index described by $\mathbf{T}^{(1)}$ in (42), depending on the mean phonon position operator

$$\langle q(0) \rangle_t = \frac{\tau}{2V m \Omega} \gamma^{pump} \sin(\Omega t). \quad (65)$$

The transmitted light can be computed as discussed before but, unlike for the pump pulse, due to the non-vanishing first order contribution from the Raman process, we can neglect second order contributions. Explicitly, one finds

$$\langle I_{\lambda j}(\tau) \rangle_t = |\tilde{\alpha}_{\lambda j}^{probe}|^2 + \tau \frac{V_S}{2V m \Omega} \sum_{\lambda} \chi_{\lambda\lambda}^{(1)} \omega_j |\tilde{\alpha}_{\lambda j}^{probe}| \left(|\tilde{\alpha}_{\lambda j + \frac{\Omega}{8}}^{probe}| - |\tilde{\alpha}_{\lambda j - \frac{\Omega}{8}}^{probe}| \right) \langle p(0) \rangle_t, \quad (66)$$

where

$$\langle p(0) \rangle_t = i \sqrt{\frac{m\Omega}{2V_S}} (b^\dagger - b)_t = \frac{\tau}{2V} \gamma^{pump} \cos(\Omega t). \quad (67)$$

By looking at the expressions (65) and (67) one can introduce the parameter $R^2 = \langle p(0) \rangle_t^2 + m^2 \Omega^2 \langle q(0) \rangle_t^2$, related to the vibrational energy, and recast the initial conditions for the probe interaction as in the main text

$$\begin{cases} t < 0, & \langle q(0) \rangle_t = \langle p(0) \rangle_t = 0 \\ t > 0, & \langle q(0) \rangle_t = \frac{R}{m\Omega} \sin(\Omega t), \quad \langle p(0) \rangle_t = R \cos(\Omega t). \end{cases} \quad (68)$$

Moreover, the action of the refraction matrix according to (62), returns

$$\langle I_{xj}(\tau) \rangle_t \simeq C_{xx}^2(t) |\alpha_j^{probe}|^2 \quad (69)$$

$$+ \tau \frac{V_S}{2Vm\Omega} C_{xx}(t) \left(C_{xx}(t) \chi_{xx}^{(1)} + C_{xy}(t) \chi_{xy}^{(1)} \right) \omega_j |\alpha_j^{probe}| \left(|\alpha_{j+\frac{\Omega}{8}}^{probe}| - |\alpha_{j-\frac{\Omega}{8}}^{probe}| \right) \langle p(0) \rangle_t \quad (70)$$

$$\langle I_{yj}(\tau) \rangle_t \simeq C_{yx}^2(t) |\alpha_j^{probe}|^2 \quad (71)$$

$$+ \tau \frac{V_S}{2Vm\Omega} C_{yx}(t) \left(C_{yx}(t) \chi_{yy}^{(1)} + C_{xx}(t) \chi_{xy}^{(1)} \right) \omega_j |\alpha_j^{probe}| \left(|\alpha_{j+\frac{\Omega}{8}}^{probe}| - |\alpha_{j-\frac{\Omega}{8}}^{probe}| \right) \langle p(0) \rangle_t. \quad (72)$$

The matrix $\mathbf{C}(t)$ can be expanded up to first order in the phononic modulation: $\mathbf{C}(t) = \mathbf{C}^{(0)} + \mathbf{C}^{(1)} \langle q(0) \rangle_t$. Therefore, keeping only linear contributions in the vibrational expectations, the term in (69) can be conveniently rewritten as follows

$$|\alpha_{xj}|^2 C_{xx}^2(t) \simeq |\alpha_{xj}|^2 \left(\left(C_{xx}^{(0)} \right)^2 + 2 C_{xx}^{(0)} C_{xx}^{(1)} \langle q(0) \rangle_t \right). \quad (73)$$

This term corresponds to the equilibrium transmission (zeroth order) plus the LRM contribution due to the matrix $\mathbf{C}^{(1)}$. Instead, the ISRS effect is described by the term in (70) that, under the same assumptions, reads

$$\tau \frac{V_S}{2Vm\Omega} C_{xx}^{(0)} \left(C_{xx}^{(0)} \chi_{xx}^{(1)} + C_{xy}^{(0)} \chi_{xy}^{(1)} \right) \omega_j |\alpha_j^{probe}| \left(|\alpha_{j+\frac{\Omega}{8}}^{probe}| - |\alpha_{j-\frac{\Omega}{8}}^{probe}| \right) \langle p(0) \rangle_t. \quad (74)$$

From this expression one can easily outline the difference between the LRM effect and the ISRS effect. In particular, only the second one modifies the relative intensity of different spectral components. Moreover, concerning the time-dependence, the two modulations oscillate with the same frequency but with different phases. In particular, the LRM contribution is driven by the phonon position while the ISRS effect is proportional to the momentum. The very same treatment can be used for (71) and (72).

In order to simplify the expressions above and make a comparison with the experiment, in the following we consider this particular form for the zeroth order refraction matrix $\mathbf{T}^{(0)}$ in (42):

$$\mathbf{T}^{(0)} = \begin{pmatrix} T_{xx}^{(0)} & T_{xy}^{(0)} \\ T_{xy}^{(0)} & T_{xx}^{(0)} \end{pmatrix}, \quad (75)$$

where $T_{xx}^{(0)}$ and $T_{xy}^{(0)}$ are real parameters accounting for how much of an incident transmitted polarization is depleted in favour of a reflected one.

QUARTZ

Three different phonons of quartz are studied with our setup, indicated in brief as A , E_L and E_T . The matrix $\chi^{(1)}$ has therefore a different structure depending on the specific phonon excited. In particular, one has

$$A : \chi^{(1)} = \begin{pmatrix} a & 0 \\ 0 & a \end{pmatrix}, \quad (76)$$

$$E_L : \chi^{(1)} = \begin{pmatrix} c_L & 0 \\ 0 & -c_L \end{pmatrix}, \quad (77)$$

$$E_T : \chi^{(1)} = \begin{pmatrix} 0 & -c_T \\ -c_T & 0 \end{pmatrix}. \quad (78)$$

With the previous assumptions on the structure of the matrices \mathbf{T} , one can compute the matrix $\mathbf{C} = \cos(\mathbf{T})$ in the three cases. It is sufficient to notice that in any case the most general structure for the matrix \mathbf{T} is the following

$$\mathbf{T} = \begin{pmatrix} u+v & w \\ w & u-v \end{pmatrix} = \left(u + \sqrt{w^2 + v^2} \right) \mathbf{Q}_1 + \left(u - \sqrt{w^2 + v^2} \right) \mathbf{Q}_2, \quad (79)$$

where the orthogonal projectors \mathbf{Q}_1 and \mathbf{Q}_2 , satisfying $\mathbf{Q}_1\mathbf{Q}_2 = \mathbf{Q}_2\mathbf{Q}_1 = 0$ and $\mathbf{Q}_1^2 = \mathbf{Q}_2^2 = \mathbf{1}$, explicitly read

$$\mathbf{Q}_1 = \frac{1}{w^2 + (\sqrt{w^2 + v^2} - v)^2} \begin{pmatrix} 1 & w(\sqrt{w^2 + v^2} - v) \\ w(\sqrt{w^2 + v^2} - v) & (\sqrt{w^2 + v^2} - v)^2 \end{pmatrix}, \quad (80)$$

$$\mathbf{Q}_2 = \frac{1}{w^2 + (\sqrt{w^2 + v^2} - v)^2} \begin{pmatrix} (\sqrt{w^2 + v^2} - v)^2 & -w(\sqrt{w^2 + v^2} - v) \\ -w(\sqrt{w^2 + v^2} - v) & w^2 \end{pmatrix}. \quad (81)$$

These expressions allow one to determine explicitly the matrix $\cos(\mathbf{T})$ and to compute the relevant terms contributing to the intensity. Indeed, from (79) it turns out that

$$\cos(\mathbf{T}) = \cos\left(u + \sqrt{w^2 + v^2}\right) \mathbf{Q}_1 + \cos\left(u - \sqrt{w^2 + v^2}\right) \mathbf{Q}_2 \quad (82)$$

and it is sufficient to substitute the variables u, v, w with the relevant quantities for the three phononic modes.

In the end, the coefficients $C_{nm}^{(0)}$ and $C_{nm}^{(1)}$ are computed explicitly and, neglecting terms of order $T_{xy}^{(0)}\tau$ and $(T_{xy}^{(0)})^2$, one gets the following expressions for the transmitted probe light

$$\langle I_{xj}(\tau) \rangle_t \simeq \cos^2(T_{xx}^{(0)}) |\alpha_j^{probe}|^2 + \langle q(0) \rangle_t |\alpha_j^{probe}|^2 F_{ref}^x \quad (83)$$

$$+ \omega_j \frac{V_S}{2Vm\Omega} |\alpha_j^{probe}| \left(|\alpha_{j+\frac{\Omega}{8}}^{probe}| - |\alpha_{j-\frac{\Omega}{8}}^{probe}| \right) \langle p(0) \rangle_t F_{Ram}^x(\tau), \quad (84)$$

$$\langle I_{yj}(\tau) \rangle_t \simeq \langle q(0) \rangle_t |\alpha_j^{probe}|^2 F_{ref}^y \quad (85)$$

$$+ \omega_j \frac{V_S}{2Vm\Omega} |\alpha_j^{probe}| \left(|\alpha_{j+\frac{\Omega}{8}}^{probe}| - |\alpha_{j-\frac{\Omega}{8}}^{probe}| \right) \langle p(0) \rangle_t F_{Ram}^y(\tau), \quad (86)$$

where the coefficients $F_{ref}^{x,y}$ and $F_{Ram}^{x,y}(\tau)$ are given by

$$\left\{ \begin{array}{ll} A : & \begin{array}{l} F_{ref}^x = -ak_T \sin(2T_{xx}^{(0)}) \\ F_{ref}^y = 0 \end{array} & \begin{array}{l} F_{Ram}^x(\tau) = a\tau \cos^2(T_{xx}^{(0)}) \\ F_{Ram}^y(\tau) = 0 \end{array} \\ E_L : & \begin{array}{l} F_{ref}^x = -c_L k_T \sin(2T_{xx}^{(0)}) \\ F_{ref}^y = 0 \end{array} & \begin{array}{l} F_{Ram}^x(\tau) = c_L \tau \cos^2(T_{xx}^{(0)}) \\ F_{Ram}^y(\tau) = 0 \end{array} \\ E_T : & \begin{array}{l} F_{ref}^x = c_T k_T 2T_{xy}^{(0)} \cos^2(T_{xx}^{(0)}) \\ F_{ref}^y = -c_T k_T 2T_{xy}^{(0)} \sin^2(T_{xx}^{(0)}) \end{array} & \begin{array}{l} F_{Ram}^x(\tau) = 0 \\ F_{Ram}^y(\tau) = 0 \end{array} \end{array} \right.$$

In order to emphasize the dependence on the angle between the pump polarization and the probe one, we consider γ^{pump} for the three different phonons. Since we neglected contributions of order $T_{xy}^{(0)}\tau$, only the diagonal elements of $\mathbf{T}^{(0)}$ appear in γ^{pump} that explicitly reads

$$\begin{aligned} A : \quad \gamma^{pump} &= a \cos^2(T_{xx}^{(0)}) \sum_j \omega_j |\alpha_j^{pump}| |\alpha_{j+\frac{\Omega}{8}}^{pump}| \\ E_L : \quad \gamma^{pump} &= c_L \cos(2\theta) \cos^2(T_{xx}^{(0)}) \sum_j \omega_j |\alpha_j^{pump}| |\alpha_{j+\frac{\Omega}{8}}^{pump}| \\ E_T : \quad \gamma^{pump} &= -c_T \sin(2\theta) \cos^2(T_{xx}^{(0)}) \sum_j \omega_j |\alpha_j^{pump}| |\alpha_{j+\frac{\Omega}{8}}^{pump}| \end{aligned}$$

Therefore, if the pump pulse is polarized at 45° one can excite the modes A and E_T but not E_L . Conversely, if the pump is polarized at 0° the two modes A and E_L are excited. These results are used in the main text to compare the model predictions with the experimental evidence. In the following, we plot the theoretical transmitted intensity in the two different settings discussed in the main text. In particular, the theoretical plots in Figs. 6 and 8 refer to the cases where

1. one measures the transmitted probe light with polarization along the y axis and the pump photons are polarized at 45° . It has to be compared with the experimental one in the main text that we report here for convenience (Fig. 7): the theoretical model correctly predicts that only the LRM effect is detectable in this pump-probe polarization configuration;
2. pump and probe polarizations are parallel to the x axis, both A and E_L modes contribute, and one measures the x -polarized transmitted light. One sees in Fig. 8 that both ISRS and LRM processes are visible. This is consistent with the experimental evidence reported in Fig. 9.

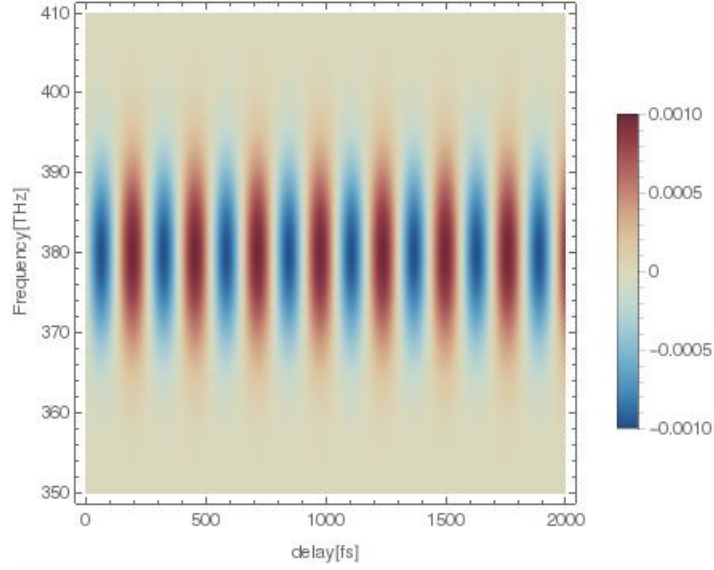


FIG. 6. Spectral modulation vs delay in the ($\lambda = y, \theta = 45^\circ$) configuration (Theoretical plot).

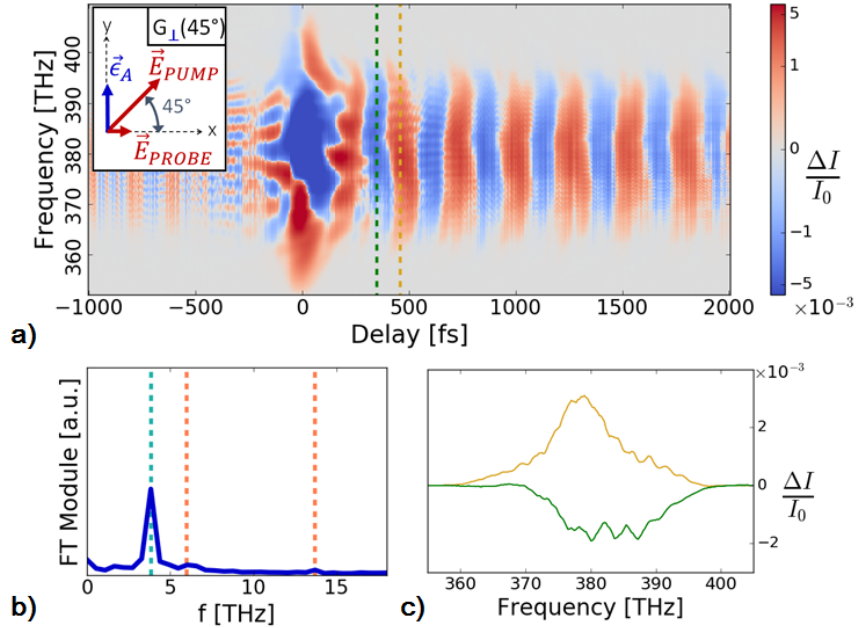


FIG. 7. a) Spectral modulation vs delay in the ($\lambda = y, \theta = 45^\circ$) configuration (insert) is presented. b) FT: only the 4 THz E_T phonon is detected. c) The transmittivity modulation is selected at $t = 351$ fs (green) and $t = 458$ fs (gold). As expected for the refractive modulation the transmittivity change has the same sign for the whole spectrum.

EXPERIMENTAL DETAILS

In the main text, we report the results of pump&probe frequency-resolved, polarization dependent, measurements on α -quartz. In this section, a brief description of the experimental setup is given (Fig.10).

The pulsed laser source is characterized by 800 nm wavelength, 5 kHz repetition rate and 40 fs pulse duration. The output is split in order to obtain the pump and probe beams. The relative delay between the two is controlled by means of a translation stage on the pump path (delay resolution 6.7 fs). With a second beam splitter, a reference copy of the incident probe pulse is obtained, which is useful to remove noise and distinguish in the transmitted signal

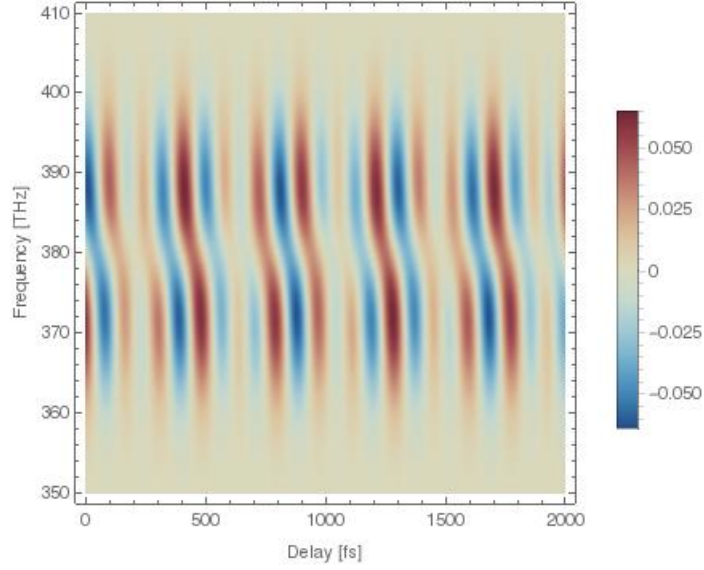


FIG. 8. Spectral modulation vs delay in the ($\lambda = x$, $\theta = 0^\circ$) configuration (Theoretical plot).

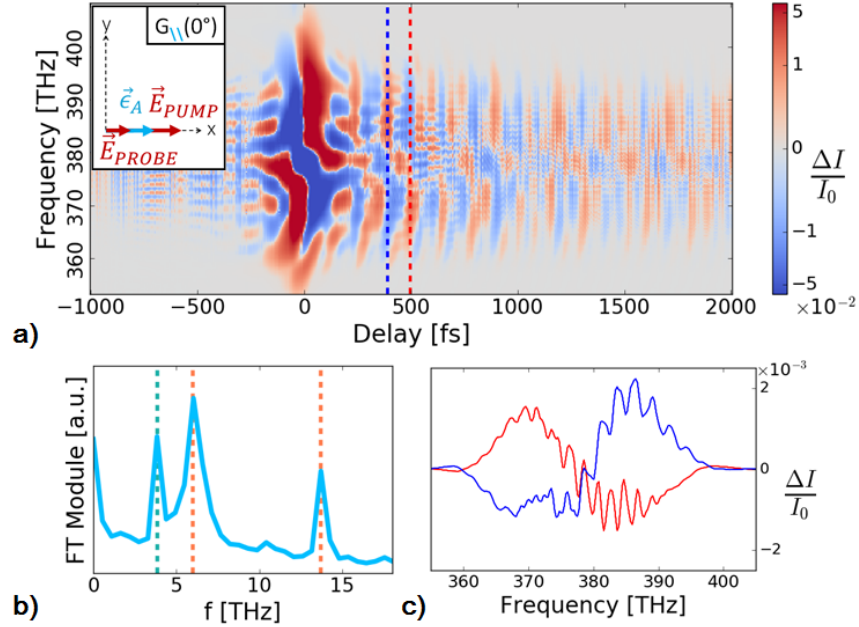


FIG. 9. Results depending on the relative orientation between pump and probe polarizations and analyzer direction. a) Spectral modulation vs delay in the ($\lambda = x$, $\theta = 0^\circ$) configuration (insert) is presented. b) FT: 4 THz E_L phonon is detected, together with 6 THz and 14 THz A symmetry modes. c) The transmittivity modulation is selected at $t = 391$ fs (blue) and $t = 498$ fs (red). Spectral shifts resulting from ISRS are observed.

only the relevant information about the interaction processes with the sample.

Half-wave plates and polarizers control the relative orientation θ of pump-probe polarizations. A polarizer is also added after the sample (analyzer) to select the observed polarization λ .

The α -quartz sample is 1 mm thick and the employed pump and probe fluences are respectively 0.8 mJ/cm^2 and $0.7 \mu\text{J/cm}^2$.

Single-shot wavelength-resolved spectra of both probe beams are measured through a pair of transmission spectrometers, each provided with a linear array of 256 photodiodes, with frequency resolution 0.15 THz. The spectrum associated with a single time delay is the average over about 1000 single pulse acquisitions.

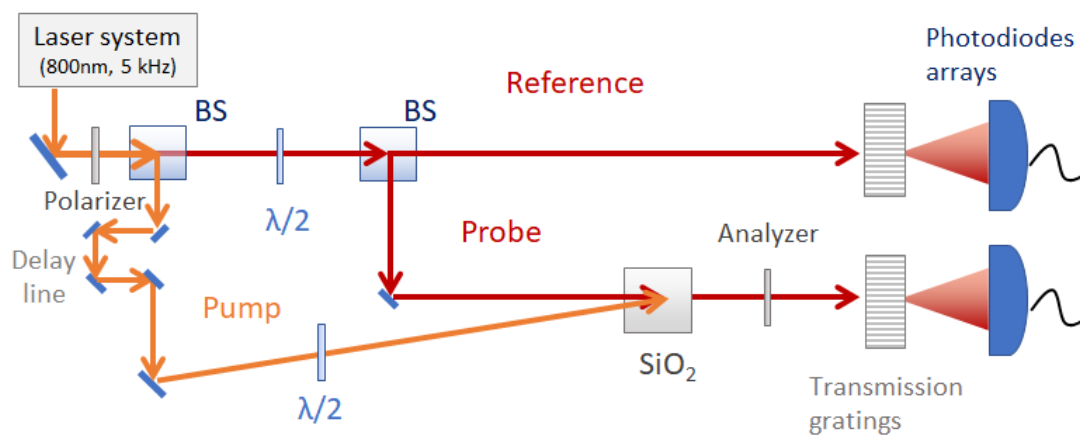


FIG. 10. Scheme of the experimental setup.